

Results of a gallium phosphide photovoltaic junction with an AR coating under concentration of natural sunlight

C.R. Allen, J.M. Woodall*, J.-H. Jeon

Electrical and Computer Engineering, Purdue University, West Lafayette, IN 47907-2035, United States

ARTICLE INFO

Article history:

Received 15 October 2010

Received in revised form

10 May 2011

Accepted 13 May 2011

Keywords:

Anti-reflection

Gallium phosphide

PMMA

CPV

ABSTRACT

A gallium phosphide (GaP) photovoltaic junction is grown by molecular beam epitaxy (MBE) on a GaP substrate. An anti-reflection coating of polymethyl methacrylate (PMMA) is applied and the cell is measured under concentrations of $1\times$ and $10.7\times$ in an outdoor setting. Efficiencies up to 2.6% and open circuit voltages up to 1.57 V are reported.

© 2011 Elsevier B.V. All rights reserved.

1. Introduction

The global interest in effective solar energy conversion is gaining, with many new solar power plants being built every year. In order to reach efficiencies over 35%, solar cells must be multi-junction devices. The overall efficiency of these multi-junction devices depends heavily on the individual efficiencies of each junction. Recently, in the effort to maximize solar cell performance, GaP junctions grown by LPE [1,2] and MBE [3], as well as simulation [4], have been investigated for use in multi-junction systems. With a bandgap of 2.26 eV at room temperature, GaP is sub-optimal compared to the desired 2.4 eV bandgap for a top cell. However, lacking an economic 2.4 eV top junction, the difference in maximum efficiency when using a GaP cell is practically negligible for a multi-junction system [1].

In order to investigate the effects of concentration on a GaP junction, PMMA can be used as a simple AR coating. PMMA was chosen because it can be spun smoothly using simple processing techniques in very thin layers with readily available components [5]. It is also soft enough to easily probe through for electrical characterization. A disadvantage of PMMA is yellowing and cracking that can occur, though this is expected to happen over timeframes on the length of months [6].

This work investigates the performance of a GaP n–p junction with a PMMA anti-reflection coating under concentration in an outdoor environment.

2. Methods

2.1. Calculations

In order to reduce the amount of light that is reflected off the front surface, a $\lambda/4n$ thick layer is added to the front of the device. This layer is known as an anti-reflection (AR) coating. Ideally, the AR coating's index of refraction will be equal to the square root of GaP's index of refraction. An ideal material would have an index of refraction of approximately 1.86 in the 300–550 nm range. Since the index of refraction varies as a function of photon wavelength, the thickness of an AR coating must be tailored to a particular wavelength.

Transmission line theory can be used to calculate the reflection off the front surface if we assume normal incident plane waves for [7]. Using Eq. (1), the reflection can be calculated where η is the wave impedance as defined in Eqs. (2) and (4). The complex permittivity and permeability of the material are represented by ϵ and μ , respectively, and d is the thickness of the AR coating:

$$R = \left| \frac{\eta_{\text{in}} - \eta_0}{\eta_{\text{in}} + \eta_0} \right|^2 \quad (1)$$

$$\eta_{\text{in}} = \eta_{\text{PMMA}} \frac{\eta_{\text{GaP}} + \eta_{\text{PMMA}} \tanh \gamma d}{\eta_{\text{PMMA}} + \eta_{\text{GaP}} \tanh \gamma d} \quad (2)$$

$$\gamma = i\omega \sqrt{\mu \epsilon} \quad (3)$$

$$\eta = \sqrt{\frac{\mu}{\epsilon}} \quad (4)$$

* Corresponding author. Tel.: +1 7654943479; fax: +1 7654946440
E-mail address: woodall@purdue.edu (J.M. Woodall).

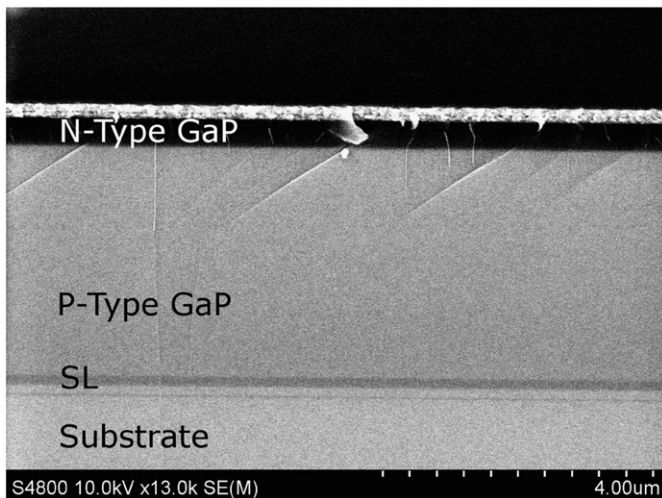


Fig. 1. Cross sectional SEM image of GaP p–n junction. The metal contact is seen on top, followed by the n-type emitter, and the p-type base. The AlGaP–GaP superlattice is seen as a dark band near the substrate. A thin growth barrier layer is present between the substrate and superlattice. Irregular textures on the cross sectional facet are artifacts from cleaving.

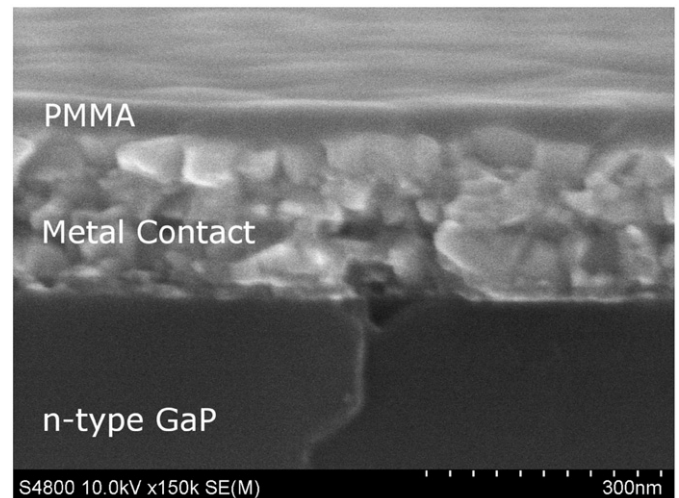


Fig. 2. Cross sectional SEM image of PMMA coating over metal contact. The PMMA can clearly be seen on top of the metal contact. Contact was made to the device by poking the probe through the PMMA.

Using data for the index of refraction of PMMA from CYRO Industries in a technical report by Ispirian et al. [8], estimates for the surface reflection can be made when the AR coating is present. Fig. 4 shows the reflection expected without an AR coating, and the reflection assuming a 75 nm thick layer of PMMA and normal light incidence. A thickness of 75 nm corresponds to approximately $\lambda/4n$ for PMMA at 450 nm.

2.2. Growth

GaP was grown on a GaP substrate by MBE. A superlattice of AlGaP–GaP was grown on the rear surface in an attempt to block the diffusion of impurities from the substrate. It also provides good contrast when imaging via SEM as seen in Fig. 1. A 4.5 μm p-type GaP layer, doped $1e17$ with Be, is grown on top of the superlattice, followed by a 500 nm n-type GaP layer doped $1e18$ with Si. A 10 nm thick layer of n-type GaP doped $1e20$ with Si is used as a cap layer.

2.3. Fabrication

Cell mesas were defined using an aqua regia etch with AZ1813 defining the mesa. Pd–Zn–Pd contacts were used to contact the device from the front of the base layer [9]. Au–Ge–Ni contacts were defined in a grid pattern on the top of the mesas. AZ1827 was used as the sacrificial photoresist for liftoff of the contacts.

The anti-reflection coating procedure is based on the work by Walsh and Franses [5]. The sample is solvent cleaned with acetone and isopropanol. The sample is then oven dried at 120 °C for 20 min. A solution of 2 wt% $\bar{M}_w=97,000$ and $\bar{M}_n=44,700$ PMMA in toluene is spun onto the sample at 1000 RPM. The coating is cured on a hotplate at 140 °C for 1 h. The PMMA coating can be easily removed with toluene or acetone. The PMMA coating is applied after etching, metal deposition, and annealing is completed, as seen in Fig. 2.

2.4. Characterization

Concentration measurements were taken on March 16, 2010, at approximately 4 pm EDT near the south-west corner of the Birck Nanotechnology Center. A Keithley 2400 sourcemeter, connected to a computer for data acquisition, was placed on a mobile

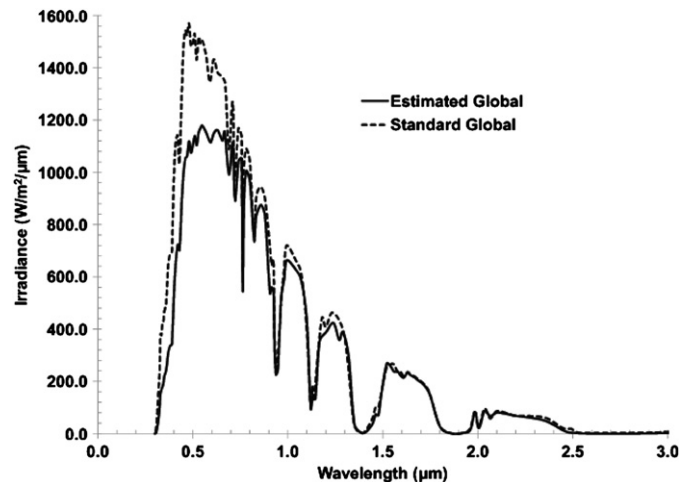


Fig. 3. AM1.5 (dash) compared to the Bird model estimation of the input spectrum (solid) properly adjusted for time of day and location. Both spectrums assume a cloudless day.

cart with a small probe platform. The probe platform was angled toward the sun such that the surface of the cell was normal to the sunlight. For concentration, a UV-AR-coated convex lens was used to concentrate sunlight on the cell.

The estimated input spectrum is seen in Fig. 3, generated using the Bird model [10], which is available on the NREL website in Excel format [11]. It assumes a cloudless day, which is not completely accurate for the time of measurement. The direct component of the simulated spectrum is used for the concentration measurement simulation, whereas simulation of the non-concentrated measurement is conducted with a global-tilt spectrum (direct and diffuse).

3. Results

Walsh and Franses [5] note variations in the index of refraction at 632.8 nm by up to a few percent. Švorčík et al. [12] also reported significant variations in index of refraction at low thicknesses. The wavelength region of interest for GaP photo-voltaics is approximately 300–600 nm. This range typically has

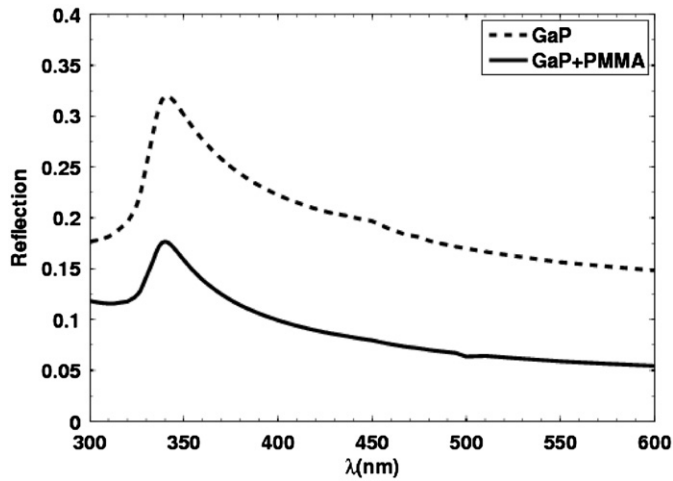


Fig. 4. Estimated reflections of bare GaP (dash) and PMMA coated GaP (solid).

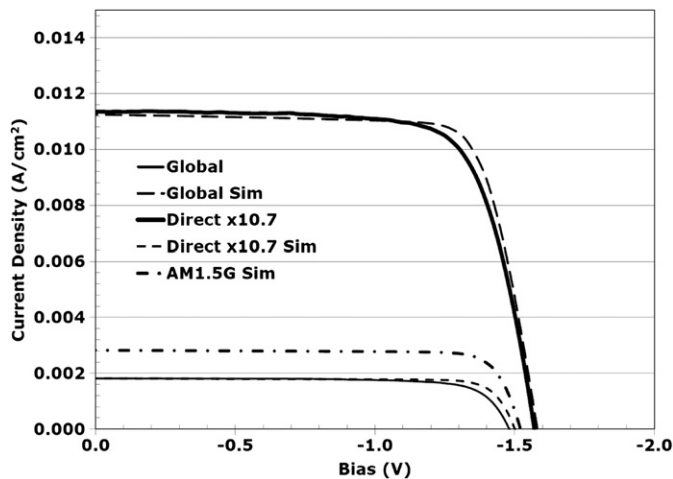


Fig. 5. Measured (solid) and simulated (broken lines) *IV* curves of concentrations of a 1 × global spectrum, 10.7 × direct spectrum, and the AM1.5 global spectrum. The 1 × and 10.7 × spectrums were calculated from the Bird model.

Table 1

Performance of the cell as a function of concentration.

Concentration	FF	V_{oc} (V)	J_{sc} (mA/cm ²)	Efficiency (%)
1 (global)	0.77	1.48	1.81	2.60
10.7 (direct)	0.74	1.57	11.35	2.05

significant changes in index of refraction for any material. Thus the reflection across this spectrum changes significantly, and predictions may yield only a good estimate.

The resulting *IV* curves for the GaP cell with AR coating can be seen in Fig. 5. These results are summarized in Table 1. The clouds were sparse enough to provide only a small error in light generated current during a measurement. Thus the results in Table 1, which assume a cloudless day, represent a slight underestimation of the actual cell efficiency.

Typically an increase in solar concentration yields higher efficiencies. As can be seen in Table 1, an increase in concentration does not yield an increase in efficiency. This can be attributed to the deterioration of the fill factor caused by series resistance. This effect can be seen in the light-biased *IV* curves in Fig. 5.

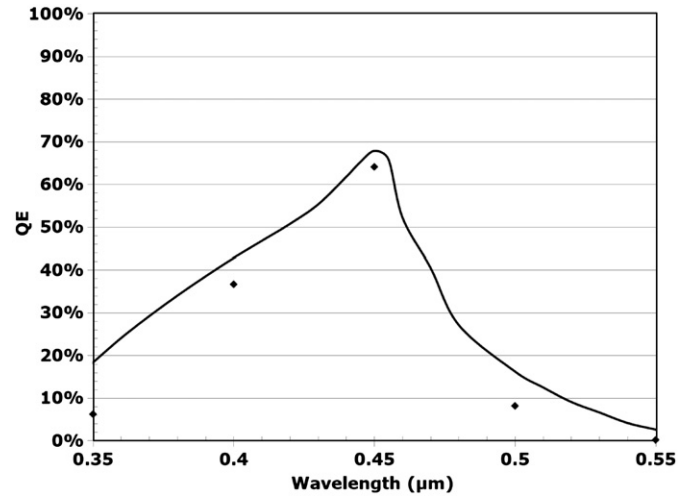


Fig. 6. Measured (dots) and simulated (line) reflection-compensated quantum efficiencies.

Previous results [3] predict an efficiency of 2.6% vs AM1.5g for a good AR coating and eliminating series and shunt resistances. This cell performed better than expected by achieving 2.6% while still having significant series resistance and an imperfect AR coating. From our prior work, the predicted V_{oc} and J_{sc} of a device with an ideal AR coating and without series or shunt resistances are 1.57 V and 1.96 mA/cm², respectively. Those prior predictions assume an input spectrum of AM1.5g. The simulation used in the prior work can be modified to give the results of V_{oc} =1.52 V, J_{sc} =2.82 mA/cm², and FF=0.82, yielding an efficiency of 3.53% as seen in Fig. 5. The increase in efficiency can be attributed largely to the short circuit current increase from a significant improvement of the peak quantum efficiency at 450 nm, as seen in Fig. 6. The application of PMMA does not improve the front surface recombination. As such, a proper front surface barrier still needs to be investigated. The major factors that restrict performance are still front surface recombination and recombination in the p-type base, whose effects have been investigated previously [3].

4. Conclusions

An AR coating of PMMA is applied to a GaP photovoltaic junction. Measurements are taken in natural sunlight at 1 × and 10.7 × concentrations. An efficiency of 2.6% is obtained. Concentration yields an increase in V_{oc} up to 1.57 V, but efficiency decreases due to series resistance. The areas of improvement remain the need for a good front surface barrier and need to improve p-type minority carrier lifetime.

References

- [1] X.Lu, S.R. Huang, M. Diaz, R.L. Opila, A. Barnett, Wide bandgap gallium phosphide solar cells for multi-junction solar cell system, in: Proceedings of the 35th IEEE PVSC, Honolulu, Hawaii, 2010, pp. 002079–002083.
- [2] O. Sulima et al., High-temperature AlGaP/GaP solar cells for NASA Space Missions, in: Proceedings of the third World Conference on PVE Con, 2003, pp. 737–740.
- [3] C.R. Allen, J.-H. Jeon, J.M. Woodall, Simulation assisted design of a gallium phosphide n-p photovoltaic junction, *Sol. Energy Mater. Sol. Cells* 94 (5) (May 2010) 865–868.
- [4] I. Bhattacharya S.Y. Foo, Effects of gallium-phosphide and indium-gallium-antimonide semiconductor materials on photon absorption of multi-junction solar cells, in: Proceedings of IEEE SoutheastCon 2010, Concord, NC, 2010, pp. 316–319.

- [5] C.B. Walsh, E.I. Franses, Ultrathin PPMA films spin-coated from toluene solutions, *Thin Solid Films* 429 (1–2) (2003) 71–76.
- [6] David C. Miller, Lynn M. Gedvilas, Bobby To, Cheryl E. Kennedy, Sarah R. Kurtz, Durability of poly(methyl methacrylate) lenses used in concentrating photovoltaic modules, in: *Proceedings of SPIE*, vol. 7773, San Diego, 2010, p. 777303.
- [7] S. Ramo, J.R. Whinnery, T.V. Duzer, *Fields and Waves in Communication Electronics*, John Wiley & Sons, Inc., Hoboken, NJ, 1994, pp. 274–320.
- [8] M. Ispirian, S. Karabekyan, R. Eckmann, Measurements of transmission of plastic, Technical report 1997, pp. 1–16.
- [9] L. Baojun, L. Enke, Z. Fujia, Pd/Zn/Pd ohmic contacts to p-type GaP, *Solid-State Electron.* 41 (6) (1997) 917–920.
- [10] R.E. Bird, C.J. Riordan, Simple solar spectral model for direct and diffuse irradiance on horizontal and tilted planes at the earth's surface for cloudless atmospheres, *J. Clim. Appl. Meteorol.* 25 (January 1986) 87–97.
- [11] R. Bird, C. Riordan, D. Myers. RReDC Solar Models: SPCTRAL2 [online] <<http://rredc.nrel.gov/solar/models/spectral/SPCTRAL2/>>, 2010.
- [12] V. Švorčík, O. Lyutakov, I. Huttel, Thickness dependence of refractive index and optical gap of PMMA layers prepared under electric field, *J. Mater. Sci.: Mater. Electron.* 19 (4) (2007) 363–367.